On the effect of poly(3-hexylthiophene) regioregularity on inkjet printed organic solar cells†

Claudia N. Hoth,[ab] Stelios A. Choulis,[c] Pavel Schilinsky[a] and Christoph J. Brabec[a]

Received 6th January 2009, Accepted 27th March 2009
First published as an Advance Article on the web 7th May 2009
DOI: 10.1039/b823495g

We investigate the impact of P3HT regioregularity on the performance of bulk heterojunction solar cells with inkjet printed P3HT:PCBM layers. Three polythiophenes with different regioregularities ranging from 93% up to 98% are inkjet printed from two different formulations at room temperature. It is found that the high RR-P3HT (98%) is not suitable for inkjet printing at room temperature. The fast formation of aggregates shortens the shelf life of the ink and thus, results in low reliability of the printing process, in the formation of inhomogeneous and very rough films with surface roughnesses up to 70 nm, and in a strongly reduced device performance. This phenomenon is not observed for solar cells processed *via* the doctor blading technique. Nevertheless, inkjet printing of 96% RR-P3HT:PCBM oDCB/mesitylene solutions at room temperature resulted in solar cells with 3.5% efficiency, while doctor blading of 98% RR-P3HT:PCBM oDCB/mesitylene solutions resulted in efficiencies as high as 4.4%.

Introduction

A variety of approaches has been used to solution deposit the most prominent photoactive organic materials poly(3-hexylthiophene) (P3HT) and [6,6]-phenyl C61 butyric acid methyl ester (PCBM) of bulk heterojunction (BHJ) organic solar cells (OSC). The commonly applied deposition techniques are solution-based processes such as spin coating,[1,2] doctor blading[3–5] or printing.[6,7] Due to the compatibility to roll-to-roll production, printing technologies[6,7] have gained significant attraction for organic semiconductor processing, among them screen printing,[8–12] gravure,[13,14] offset[15] and inkjet printing.[16–18] Screen, gravure and offset printing suffer from a complex master, but in contrast, inkjet printing has evolved to the most promising digital printing technology. Inkjet printing is so promising because polymer device fabrication can be easily adapted in terms of compatibility to various substrates, no-mask patterning solvents, and, reduction in waste products. A post-patterning of large-area spin coated or doctor bladed films has been demonstrated by using subsequent laser ablation[19] of the film to achieve the desired pattern, but it is unlikely to realize post-patterning of films as a commercially viable route. Owing to a two-dimensional patterning of films and the reduction of waste products and more importantly, to economize on one fabrication step namely the post-patterning, inkjet printing has a clear benefit there.

At present, bulk heterojunction solar cells based on blends of a polymer donor with a fullerene acceptor, are the materials systems with the highest reported efficiencies for printable solar cells. Efficiencies of up to 6% were certified by NREL,[20] but the performance depends critically on the properties of the materials as well as on the processing conditions affecting the blend morphology.[21–24] In this study we focus on the well-known donor-acceptor system P3HT:PCBM and discuss the correlation of material properties to performance in the case of inkjet printing. Fig. 1b shows the chemical structures of P3HT and PCBM.

The formulation of a P3HT:PCBM blend solution as well as the chemical properties of the polythiophene have a strong impact on the nature of the droplet generation, ejection process and film formation in the inkjet process. In parallel, various studies investigate the influence of molecular weight distribution of P3HT on charge carrier mobility and device performance for solution processed films.[25–27] Schilinsky *et al.* reported on improved power conversion efficiencies (PCE) for P3HTs with a number average molecular weight of greater than 10000 g mol^{-1} due to improved hole mobility accompanied by increased intermolecular ordering (pi stacking) of the P3HT phase.[27] Lately, Ballantyne *et al.* observed constant hole mobility at molecular weight ranges from 13000 to 18000 g mol^{-1}, but reduced hole mobility for molecular weight values between 34000 to 121000 g mol^{-1} due to a change in surface morphology resulting in decreased OSC device

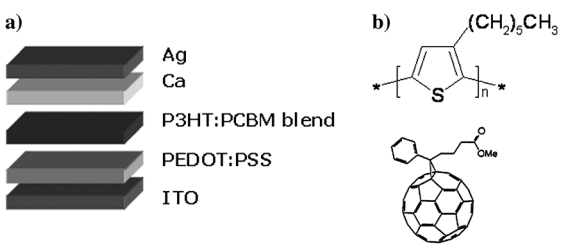

Fig. 1 a) Device architecture of the solar cell ITO/PEDOT:PSS/P3HT:PCBM blend/Ca/Ag under study. b) Chemical structures of poly(3-hexylthiophene) and [6,6]-phenyl C61 butyric acid methyl ester.

[a]*Konarka Technologies GmbH, Landgrabenstr. 94, D-90443 Nürnberg, Germany*
[b]*Department of Energy and Semiconductor Research, University of Oldenburg, D-26129 Oldenburg, Germany*
[c]*Department of Mechanical Engineering and Materials Science and Engineering, Cyprus University of Technology, 3603 Limassol, Cyprus*
† This paper is part of a *Journal of Materials Chemistry* theme issue on solar cells. Guest editors: Michael Grätzel and René Janssen.

performance.[25] Recently, Kim *et al.* attributed the improved device performance using higher regioregularity (RR), defined as the percentage of monomers adopting a head-to-tail configuration rather than head-to-head, to enhanced optical absorption and transport properties.[28] A high regioregular P3HT organizes more rodlike in planar structures, and results in the formation of well-ordered lamellar structures (crystallites) with extended conjugation leading to enhanced charge carrier mobility.[29–32] Higher RR enables closer packing of these lamellae and thus, promotes interchain alignment.[28] Due to the regioregular alignment of high RR-P3HT in solution, single chains may undergo self-assembly and interact with adjacent rods, resulting in large linked clusters and subsequent aggregation[33] between the rods of different polymer chains, also called gelation. The formation of gels in P3HT is usually attributed to the formation of physically cross-linked polymer strands. This network formation is thermoreversible, can be dissipated upon reheating accompanied by endothermic heat flow, and is therefore called gelation.[34] Gelation significantly affects the stability of the semiconductor solution in terms of a short shelf life and a low reproducibility, mainly due to an increased viscosity of a gelled formulation. Inkjet printing is very sensitive to gelling, and the photovoltaic performance of inkjet printed devices depends critically on the state of the ink to guarantee stable jetting behaviour for a reproducible printing process.

In this manuscript we discuss that inkjet printing requires a distinct material specification, which is different to the material specification of other solution-processed methods like *e.g.* blading technologies. The processing conditions, morphology and performance of inkjet printed layers depend much more strongly on the material and ink properties than for other solution processing methods. In this communication we investigate that regioregularity (RR) of P3HT, among the molecular mass distribution, has the most critical impact on ink formulation. Improper P3HT specifications provoke instable solutions, showing a limitation due to strong gelation leading to a reduced processing window as well as to insufficient reproducibility. A strong correlation between the regioregularity of the conjugated polymer and the shelf life of the blend fluid affecting the photovoltaic performance is found. The solar cell device performance is investigated for doctor bladed versus inkjet printed devices for several P3HT:PCBM blends with different P3HT regioregularity (RR). Mono-solvent approaches based on pristine tetralin are compared to two-component solvent-mixtures constituted of 68% oDCB and 32% mesitylene. More details on the individual solvent formulation can be found elsewhere.[17]

The device performance is demonstrated according to the common device configuration glass/ITO/PEDOT:PSS/active layer/Ca/Ag, as depicted in Fig. 1a. Moreover, we investigate the spectrally resolved absorption behaviour of polymer solutions with different RR-P3HT, formulated either in tetralin or oDCB/mesitylene at ambient conditions and elevated temperature.

Experimental

Materials and instrumentation

Solar cell devices were built on transparent indium tin oxide (ITO) coated glass substrates, purchased from TFD. Glasses were cleaned for 10 min in acetone and another 10 min in isopropyl alcohol in an ultrasonic bath. Before use, substrates were surface treated for 10 min in an ozone oven. Subsequently, a 60 nm thin layer of poly(3,4-ethylene dioxythiophene) doped with polystyrene sulfonic acid (PEDOT:PSS Clevios PH) was deposited by doctor blading on top of the ITO bottom electrode. After PEDOT:PSS doctor blading, samples were stored in inert atmosphere for at least two hours. The photoactive layer consists of 1 wt% P3HT blended with fullerene PCBM in a 1:1 weight ratio and either dissolved in pristine tetralin or in an ortho-dichlorobenzene/mesitylene solvent mixture. All solvents were purchased from Sigma Aldrich. The semiconductor solutions were stirred at 80 °C for at least two hours. The deposition of the active layer was done by inket printing (Fujifilm Dimatix DMP-2831) or doctor blading (Erichsen Coatmaster 509MC). A thermally evaporated Ca-Ag electrode terminated the solar cell (see Fig. 1a). Prior to evaporation of the top electrode, all devices were subjected to a thermal treatment at 140 °C for 10 minutes.

The device area is defined by the overlap between the underlying ITO and the top electrode. Solar cells with an active area of typically 20 mm^2 were studied. The current density-voltage (*J-V*) characteristics were assessed with a source measurement unit SMU 2400 from Keithley in nitrogen atmosphere. The photoresponse of the solar cells was measured under AM 1.5 G illumination from a Steuernagel solar simulator at 100 mW cm^{-2}. The mismatch factor of the solar simulator for P3HT:PCBM based solar cells was determined as 0.75. Subsequently, all efficiency values in this paper were corrected for a mismatch of 0.75.

Topography analysis of thermally annealed inkjet printed and doctor bladed films coated on glass/60 nm PEDOT:PSS were performed by an atomic force microscope from NanoSurf easyScan 2 operating under ambient conditions in contact mode. For absorbance measurements, pristine donor solutions of each RR-P3HT were prepared with 1% solid content either in 100% tetralin or 68% oDCB/32% mesitylene. Solution absorption spectra were recorded with an Ocean Optics tool equipped with an attenuated total reflection (ATR) sensor from Halma at two temperatures (30 °C and 80 °C).

Results and discussion

P3HT is essentially a rigid rod polymer which gets its solubility and processability from chemically attached side groups (hexyl groups) in the 3-position of the thiophene. The chemical properties of the polythiophenes used in this study are listed in Table 1. The 93%- and 96% regioregular P3HTs have similar number average molecular weight distributions (Mn = 36 kDa and 35 kDa), with the 93% RR P3HT showing a slightly higher weight average molar mass than the 96% RR-P3HT (Mw = 72 kDa vs. 60 kDa), corresponding to a polydispersity (PD) ranging from 1.7 to 2.0. In contrast, the 98% RR-P3HT shows

Table 1 Material properties of P3HT

RR [%]	Mn [kDa]	Mw [kDa]	PD
93	36	72	2.00
96	35	60	1.70
98	21	37	1.76

a significantly lower Mn of 21 kDa and Mw of 37 kDa, but a similar PD of 1.76. Despite the lower molecular weight and its better solubility,[35] the 98% RR-P3HT has the highest tendency to aggregate and gel among these three P3HTs.

Both, tetralin and the oDCB/mesitylene mixture have excellent solvation properties for P3HT at higher temperatures. However, as soon as the temperature of the solution decreases, the ink starts gelling. The kinetics of the gelling depends critically on the chemical properties of the polymer such as the regioregularity or the molecular weight distribution but also on temperature. Agitation alone is insufficient to suppress gelation at room temperature.

We compared the gelation behaviour of three different P3HTs with respect to the time interval until gelling starts, and the occurrence of small particles in the solution. In general, we found that gelling occurs more rapidly and stronger for tetralin solutions than for oDCB/mesitylene blends. Moreover, higher RR-P3HT is shown to have a much stronger gelation tendency than lower RR-PRHT batches. At ambient temperatures, gelation can occur within 5 minutes for the 98% RR-P3HT, while the 93% RR-P3HT solution was stable for more than 75 minutes. Once the gelation is initiated and a network is formed, the ink can no longer be processed with the Dimatix inkjet printing tool. Gelation was also observed during the printing operation, being responsible for frequent nozzle clogging once the ink starts to cool down. Such rapid gelation also prevents stable ink jetting conditions. Doctor blading has a clear advantage there. Here, small amounts of fresh 80 °C hot ink is directly applied into the gap between the temperature-controlled substrate and the knife before processing. Hence, limitations due to gelling are not observed for doctor blading operation. As such, doctor blading provides a reliable reference system.

Atomic force microscopy

The materials under study differ in regioregularity. To elucidate surface topography, atomic force microscopy (AFM) was performed. The AFM images of inkjet printed and doctor bladed films based on pristine tetralin or oDCB/mesitylene are shown in Fig. 2. The inkjet printed films from tetralin (Fig. 2a) display extremely rough surfaces especially for the 98% RR (Fig. $2a_3$) P3HT:PCBM solution with a calculated rms roughness of 73 nm compared to the 96% RR (Fig. $2a_2$) and 93% RR (Fig. $2a_1$) revealing an rms of 12.3 nm and 26 nm respectively. In contrast the inkjet printed films from oDCB/mesitylene (Fig. 2b) evidence a much smoother surface topography. The rms roughness is calculated to be 3.9 nm, 7.4 nm and 41.8 nm for the 93% RR (Fig. $2b_1$), 96% RR (Fig. $2b_2$) and 98% RR P3HT (Fig. $2b_3$) respectively. The AFM images show an intimate mixing of the blend materials for the 93% RR and 96% RR-P3HT:PCBM layer. Despite that, oDCB/mesitylene is approved to result in high quality P3HT:PCBM films with decent device performance,[17,24] only rough films are gained for the 98% RR-P3HT:PCBM.

Because of the different solvent formulations as well as different regioregularities, a significant distinction in the grain size and surface roughness between the inkjet printed layers is visible. A non-uniform surface roughness could affect the interfaces of the photoactive layer and therefore, the performance of the inkjet printed device. The larger grain size of the inkjet printed tetralin P3HT:PCBM indicates strong morphological limitations. The poor morphology for tetralin films, especially for the 98% RR-P3HT:PCBM blend film is related not only to the low drying rate owing to the low vapor pressure, but also to a more pronounced aggregation during the slow drying process. In contrast, the oDCB/mesitylene films show distinct aggregation for the 98% RR P3HT:PCBM inkjet printed film, while the 93% and 96% RR blend layers yield homogeneous topographies.

As reported by Li *et al.*, slow drying is a post-processing method which may lead to high efficiency spin coated solar cells.[36] Campoy-Quiles suggested that slow drying results in higher degree of P3HT crystallites.[37] Thus, it appears sound to attribute the morphology evolution from the 93% RR to the 96% RR-P3HT:PCBM inkjet printed films to an enhanced crystallization during the slow drying process. Comparing both ink formulations used in this study, this is even more pronounced for the oDCB/mesitylene solvent formulation. We believe, that this trend is not continued for the 98% RR-P3HT:PCBM inkjet printed layer. Here, the huge surface roughness may indicate the formation of large P3HT and PCBM domains. This is even more distinct for the 98% RR blend tetralin film. In contrast, the doctor bladed oDCB/mesitylene films (Fig. 2c) reveal significantly more uniform films with low rms roughnesses in the range of a few nanometers independent of the regioregularity.

The AFM analysis indicates significant distinctions in surface roughness and grain sizes between inkjet printing and doctor blading. For both deposition techniques, the substrates were heated to 40 °C, thus, the substrate temperature should not be responsible for the discrepancies. However, the deposition and handling of the inkjet fluid is very different to doctor blading. In the doctor blading method, the ink is stored on a magnetic stirrer at 80 °C prior to processing and the hot solution is directly applied in the gap between the substrate and the knife, whereas in the inkjet printing technology, the ink is filled in a non-heated cartridge without homogeneous agitation. Prior to droplet formation, the resting ink was dwelled at ambient conditions in the cartridge and the jetting was performed with ambient temperature P3HT:PCBM solution. Independent of the solvent formulation, higher RR (98%) P3HT resulted in early nozzle clogging, while lower RR-P3HT materials resulted in reliable jetting behavior.

AFM is a sound tool to investigate the impact of solvent formulation and RR on the quality and topography of thin films. To better understand the properties and limitations of different RR-P3HT solutions, and, to understand to what extent gelling already occurs in the solution versus during the drying of the film, absorbance measurements at 30 °C and at an elevated temperature of 80 °C are performed on pristine 1 wt% P3HT solutions from tetralin and oDCB/mesitylene.

Absorbance

The optical absorption of P3HT solution was measured with an attenuated total reflection (ATR) fiber. The absorbance spectra of pristine P3HT solutions with different regioregularities based on either tetralin or oDCB/mesitylene are shown in Fig. 3. The spectra were recorded for solution temperatures of 30 °C (closed symbols) and 80 °C (open symbols). It is important to

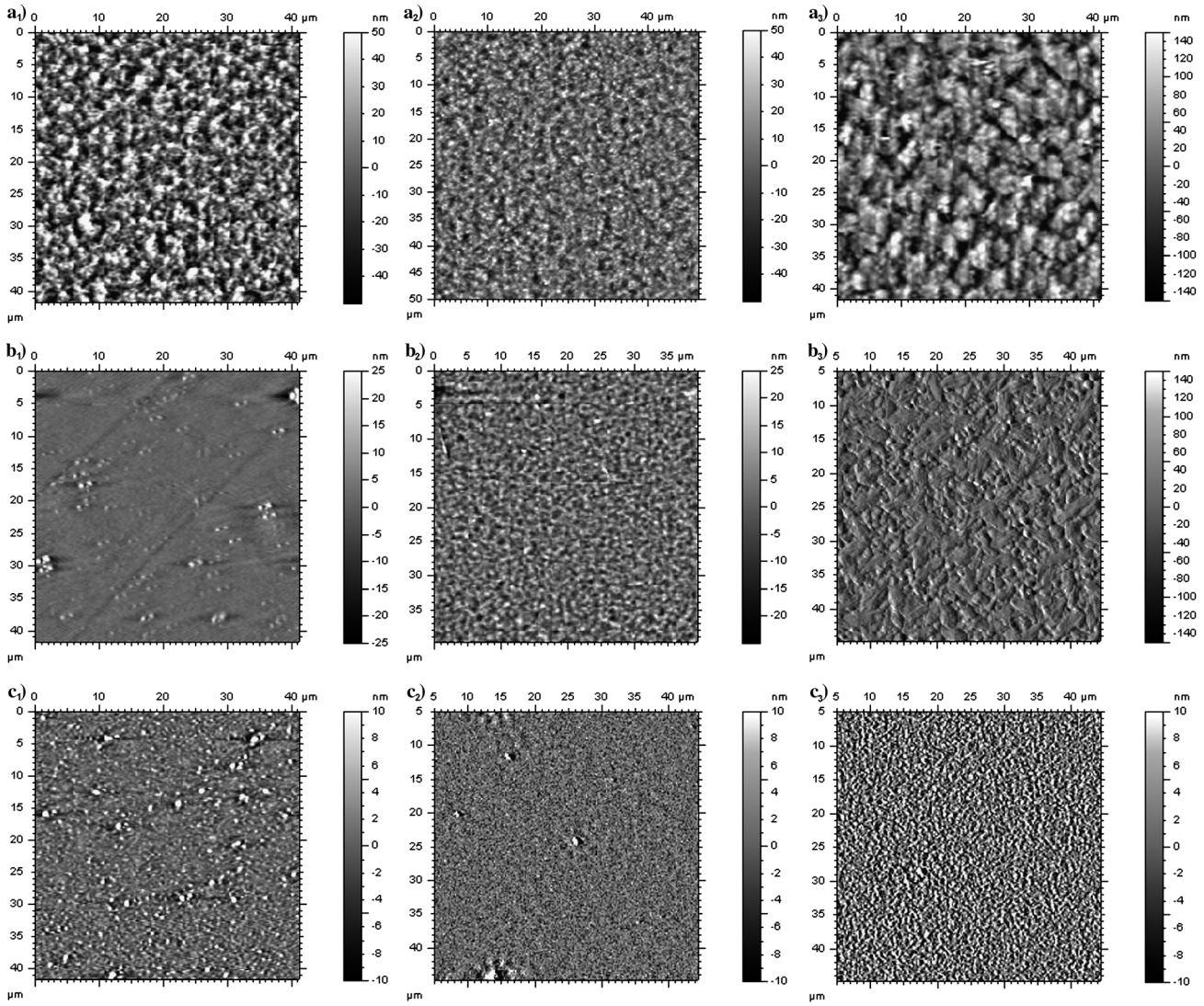

Fig. 2 Atomic force microscope images of 93%, 96% and 98% regioregular P3HT:PCBM blend films deposited by a) inkjet printing from tetralin, b) inkjet printing from oDCB/mesitylene and c) doctor blading from oDCB/mesitylene.

note, that higher RR-P3HT solutions reveal enhanced absorbance intensity. The absorbance is higher for the 30 °C solutions than for the 80 °C solutions indicating a transition in the state of aggregation from amorphous to more crystalline.[38] At ambient conditions a clear red-shift becomes visible, indicating a pi-pi transition shift of the planarized individual polymer chains.[27,29] During the transition the conjugation length increases and consequently, the electron becomes delocalized resulting in a red-shift of the absorption band.[29] The polymer backbones are more flexible at 80 °C, whereas a 30 °C solution temperature initiates aggregation of the polymer backbones. The formation of such aggregates is visually monitored by a change of the solution color from fluorescent orange to brownish. This phenomenon is most pronounced for the 98% RR-P3HT, particularly through the sharper shoulder at a wavelength of 610 nm, which has been assigned to a delocalized interchain excitation.[39] In thin films, such a shoulder was correlated with the degree of P3HT crystallinity as deduced from X-ray diffraction data.[40] Higher RR-P3HT materials tend towards more closely packing and therefore, reflect a higher intermolecular order or crystallinity. While that phenomenon is well known for thin films of P3HT, we also can observe this aggregation for the 98% RR-P3HT in solution at ambient conditions. However, these aggregates are not observed for a solution temperature of 80 °C. The kinetics of the aggregation is different for the 93%, 96% and 98% RR-P3HT solutions and is a function of solution concentration and temperature as described elsewhere.[29,30] Apart from this, not only the alkyl side chain of the polythiophene and the regioregularity affect the aggregation tendency, but also the solvent formulation and thus, the rate of solvent loss.[30,41] Correspondingly, this metastable and reversible aggregation of the P3HT solution may affect the film and morphology formation differently for different printing and coating methods.

This influence of the individual RR-P3HT:PCBM solutions based on tetralin or oDCB/mesitylene and their impact on the printing and coating reliability as well as solar cell device performance is discussed in the next section.

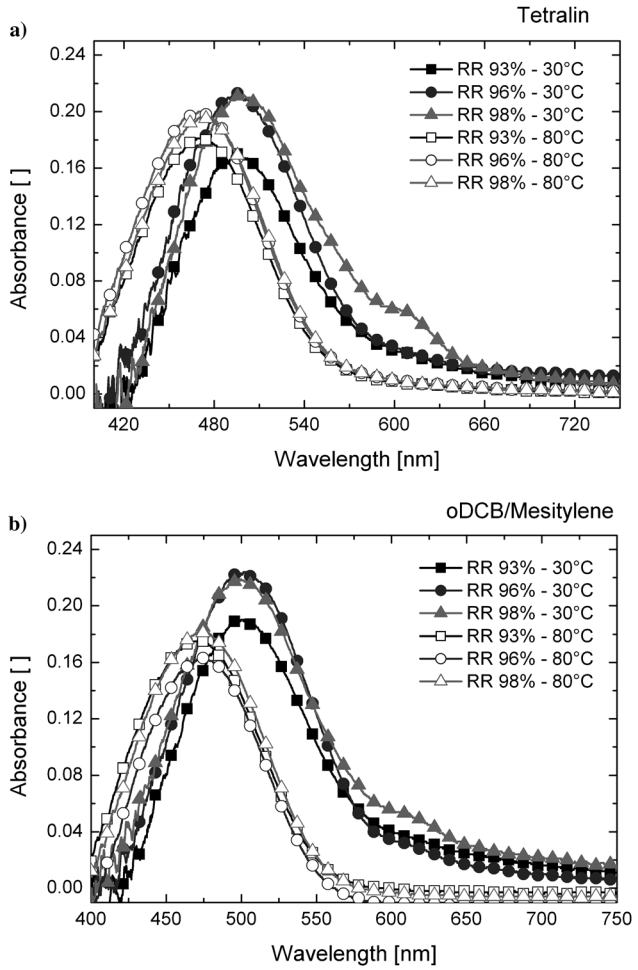

Fig. 3 Absorption spectra of pristine P3HT solutions with different regioregularities based on a) tetralin and b) oDCB/mesitylene.

Device performance

Organic photovoltaic devices were fabricated by inkjet printing and doctor blading of the P3HT:PCBM blend layer. The film thickness of the active layers ranges from 200 to 230 nm (Table 2). The film thickness of the 98% RR-P3HT:PCBM inkjet printed films could not be adjusted to 200–230 nm due to poor jetting behaviour and strong aggregation. The active layer thickness for inkjet printed 98% RR films was measured to be 300 nm. Table 2 presents the device performance parameters extracted from the analysis in terms of current density-voltage (*J-V*) characteristics and one-diode equivalent circuit for inkjet printed and doctor bladed devices under study.[42] *J-V* characterization of the inkjet printed (Fig. 4a,b) and doctor bladed (Fig. 4c,d) devices has been performed under AM1.5 illumination with 100 mW cm^{-2} and in the dark, respectively. The resulting device performances are shown in Table 2. First of all, the 93% and 96% RR-P3HT:PCBM solution demonstrated excellent jetting behaviour, whereas the 98% RR blend solution resulted in poor printing reliability as well as poor film quality. It is important to note, that the 98% RR-P3HT:PCBM ink based on tetralin was deposited onto 60 °C heated substrates due to jetting and wetting problems, while all other ink formulations were deposited onto 40 °C heated ITO/PEDOT:PSS substrates. The inkjet printed devices based on oDCB/mesitylene (closed symbols) exhibit improved device performance over the tetralin ones (open symbols) due to enhanced open circuit voltage (*Voc*) and short circuit current (*Jsc*). Improved *Voc* of oDCB/mesitylene solar cell devices arises from higher built-in potential (*Vbi*) and improved interface quality due to lower surface roughness and morphological distinctions. The origin of the reduced *Voc* of inkjet printed devices is not clear. In principle, the *Voc* of solar cells is determined by the energy gap between the acceptor LUMO and the donor HOMO. Ma *et al.* suggested that strong phase separation between the PCBM and P3HT can result in a reduction of *Voc*,[35] however, that model has not been proven so far. The much higher *Jsc* values for the inkjet printed oDCB/mesitylene solvent formulation are directly related to smoother surface topographies and enhanced morphology evolution and thus, improved charge separation.[17,24] The rough surface topographies as evidenced in the AFM images (Fig. 2a) for the tetralin based devices, 98% RR-P3HT (73 nm), 96% RR-P3HT (12.3 nm) and 93% RR-P3HT (26 nm), indicate large phase separation between P3HT and PCBM due to the low drying rate. This unfavourable morphology for inkjet printed tetralin layers is expected to be the major reason for the significantly reduced *Jsc* and is related to decreased charge separation efficiency owing to large agglomerates of donor or acceptor material. Beyond this, the reduced *Jsc* of the inkjet printed tetralin devices over the inkjet printed oDCB/mesitylene solar cells is partly explained by a first order recombination.[17]

We suggest that the limited performance of inkjet printed 93% and 96% RR tetralin devices can be at least partially attributed to

Table 2 RR-P3HT, ink formulation, device performance, surface roughness rms, device parameter extracted from the device analysis using one-diode equivalent circuit[42] and P3HT:PCBM film thickness of the inkjet printed and doctor bladed devices under study

	RR [%]	Solvent	Voc [V]	Jsc [mA/cm^2]	FF [%]	PCE [%]	rms [nm]	Vbi [V]	μT-product [cm^2/V]	thickness [nm]
inkjet printed	93	tetralin	0.45	4.7	63	1.3	26.0	0.51	5×10^{-9}	200
	93	oDCB mesitylene	0.54	8.4	64	2.9	3.9	0.59	5×10^{-9}	200
	96	tetralin	0.46	7.5	63	2.1	12.3	0.52	3×10^{-9}	200
	96	oDCB mesitylene	0.54	10.1	64	3.5	7.4	0.60	3×10^{-9}	230
	98	tetralin	0.50	4.1	35	0.7	73.0	0.55	3×10^{-9}	300
	98	oDCB mesitylene	0.41	0.5	40	0.1	41.8	0.44	5×10^{-9}	300
doctor bladed	93	oDCB mesitylene	0.58	10.4	67	4.0	3.6	0.63	4×10^{-9}	200
	96	oDCB mesitylene	0.58	11.2	64	4.1	3.7	0.63	3×10^{-9}	230
	98	oDCB mesitylene	0.56	11.7	68	4.4	7.2	0.60	4×10^{-9}	200

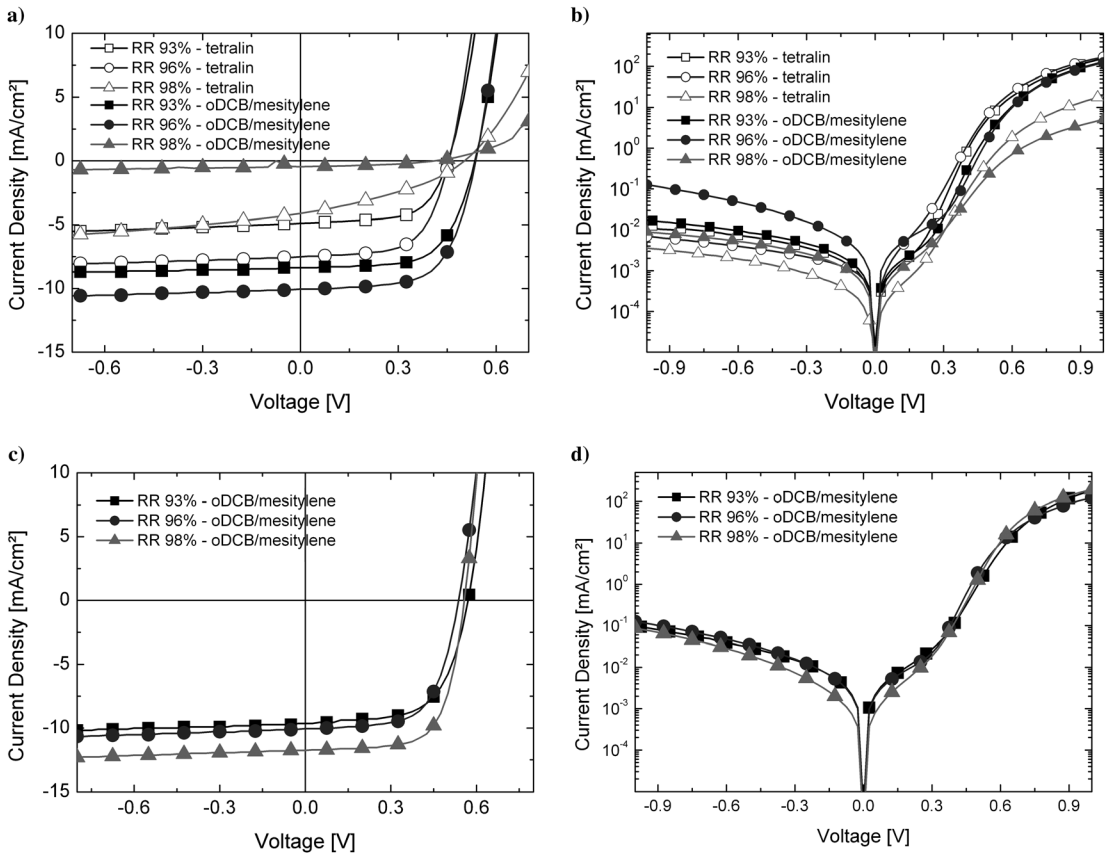

Fig. 4 Current density-voltage (*J-V*) characteristics of the different regioregular P3HT:PCBM devices based on tetralin (open symbols) or oDCB/mesitylene (closed symbols) for a) inkjet printed devices under AM 1.5 illumination with 100 mW cm^{-2} and b) inkjet printed dark *J-V* characteristics in a semi-logarithmic representation in the voltage range revealing the opening of the diode doctor bladed solar cells. c) Light *J-V* curves of doctor bladed devices based on oDCB/mesitylene under AM 1.5 illumination with 100 mW cm^{-2} and d) dark *J-V* characteristics of doctor bladed devices based on oDCB/mesitylene in a semi-logarithmic representation in the voltage range revealing the opening of the diode.

the low deposition temperatures (40 °C) at the inkjet table for the comparatively high-boiling solvent tetralin (207 °C), whereas slow drying leads to significantly stronger phase separation. Higher drying temperatures are expected to reduce this issue. In the case of the 98% RR inkjet printed devices, the tetralin based solar cell exhibits slightly better performance than the oDCB/mesitylene device, which can be attributed to the higher drying temperature (60 °C instead of 40 °C).

Independent of the solvent formulation, the devices based on 93% and 96% RR reveal high fill factors (*FF*) of 0.63–0.64. From the detailed *J-V* simulation,[42] we found that the mobility lifetime (μ-τ) product[42] (Table 2) is in the same range (3–5 × 10^{-9} cm^2 V^{-1}) for all the devices under study, indicating similar transport properties.

The doctor bladed reference devices based on oDCB/mesitylene show excellent photovoltaic performances. As reported by Kim *et al.*, higher RR leads to improved charge transport, charge carrier mobilities and light absorption.[28] Consistent with our study, enhanced current densities are observed for higher regioregularities yielding better power conversion efficiencies (PCE) for the doctor bladed solar cells. The highest device performance was achieved with the 98% RR-P3HT:PCBM blend. This device reveals a *Voc* of 560 mV, a *FF* of 0.68 and a *Jsc* of 11.7 mA cm^{-2} corresponding to a PCE of 4.4%. We would like to note that a *Jsc* of 11.7 mA cm^{-2} is an unusual high current density for P3HT:PCBM blends, which might be slightly overestimated due to our solar simulator calibration.

The major differences in the device performance between inkjet printed and doctor bladed cells are mainly due to the lower values for *Voc* and *Jsc* as discussed above. Moreover, doctor bladed devices show improved photovoltaic performance with increased RR. Beyond this observation we found, that inkjet printing requires a particular material design that ensures a high reliability of the ink without inducing process limitations. In principle, 96% RR-P3HT:PCBM inkjet printed devices show greatly improved performance over the 93% RR blend cells. However, we found that high RR (98%) materials reduce the stability of the printing fluid at ambient conditions and thus, the reliability of the jetting behaviour and printing process. It is of enormous interest to formulate inks with as high as possible RR materials for enhanced light absorption, improved mobilities and transport while not affecting the shelf life of the ink. The low device operation for the 98% RR-P3HT:PCBM formulations reveals modification of the solution in terms of aggregation that is increasing with dwell time. In contrast, the inkjet printed organic photovoltaics based on 93% and 96% RR-P3HT:PCBM blend exhibit excellent jetting behaviour and both materials are comparable and feasible to operate in high quality inks at

ambient conditions with an extended shelf life that meets the requirements for inkjet printing.

Conclusion

In this contribution, we have described bulk heterojunction solar cells with inkjet printed P3HT:PCBM layers. Three polythiophenes with different regioregularities were compared based on two solvent formulations, tetralin and oDCB/mesitylene, and deposited by inkjet printing. It is well known from the literature that high RR is needed in order to gain suitable packing of the P3HT polymer chains within the blend after annealing.[28] In the case of spin-coated films the higher the RR the better the PCE.[28] This is also observed for the doctor bladed devices discussed in this study. In contrast to our expectation the high RR-P3HT (98%) is not suitable for inkjet printing at room temperature conditions due to a short shelf life of the ink and thus, a low reliability of the jetting behaviour and printing process. At ambient conditions rapid gelling occurs in the 98% RR-P3HT:PCBM inks as a result of the higher aggregation tendency over the 93% and 96% RR materials that exhibit a long shelf life even at ambient conditions. Beyond this, the aggregation prevents a reliable jetting and leads to clogged nozzles of the printhead. To elucidate morphology, preliminary investigations were done by AFM showing a huge limitation in film quality for the inkjet printed 98% RR-P3HT:PCBM layers. Independent of the solvent formulation, the absorption spectra of pristine P3HT solutions at ambient conditions reveal strong aggregation tendencies of the 98% RR material for both solvent formulations, whereas the aggregation is suppressed for elevated temperatures. These findings indicate a clear limitation in the upper range of a high RR-P3HT:PCBM blend for inkjet printing if the fluid needs to be processed at room temperature. This phenomenon is not observed in the doctor blading technique since the hot ink is immediately applied in the gap between the coating knife and the substrate. Therefore, the RR material specification for the inkjet printing technique is a compromise between performances, and shelf life of the ink. A high photovoltaic performance of 3.5%[24] has been achieved by using a 96% RR-P3HT:PCBM blend solution based on oDCB/mesitylene, which ensures good shelf life at room temperature with respect to aggregation and thus, reliable printing.

Acknowledgements

The authors gratefully acknowledge Markus Koppe, David Waller and Prof. Jürgen Parisi for their support and valuable discussions. This study represents in part the PhD dissertation of CNH.

References

1 G. Yu and A. J. Heeger, *J. Appl. Phys.*, 1995, **78**, 4510.
2 G. Yu, J. Gao, J. C. Hummelen, F. Wudl and A. J. Heeger, *Science*, 1995, **270**, 1789.
3 C. J. Brabec, F. Padinger, J. C. Hummelen, R. A. Janssen and N. S. Sariciftci, *Synth. Met.*, 1999, **102**, 861.
4 F. Padinger, C. J. Brabec, T. Fromherz, J. C. Hummelen and N. S. Sariciftci, *Optoelectron. Rev.*, 2000, **8**, 280.
5 P. Schilinsky, C. Waldauf and C. J. Brabec, *Adv. Funct. Mater.*, 2006, **16**, 1669.
6 F. C. Krebs, *Sol. Energy Mater. Sol. Cells*, 2009, **93**, 394–412.
7 C. J. Brabec and J. R. Durrant, *MRS Bulletin*, 2008, **33**, 670–675.
8 S. E. Shaheen, R. Radspinner, N. Peyghambarian and G. E. Jabbour, *Appl. Phys. Lett.*, 2001, **79**, 2996.
9 F. C. Krebs, J. Alstrup, H. Spanggaard, K. Larsen and E. Kold, *Sol. Energy Mater. Sol. Cells*, 2004, **83**, 293.
10 T. Aernouts, P. Vanlaeke, J. Poortmans and P. Heremans, *Mater. Res. Soc. Symp. Proc.*, 2005, **836**, art. no. L3.9, 81.
11 F. C. Krebs, H. Spanggard, T. Kjaer, M. Biancardo and J. Alstrup, *Mater. Sci. Eng., B*, 2007, **138**, 106.
12 F. C. Krebs, M. Jorgensen, K. Norrman, O. Hagemann, J. Alstrup, T. D. Nielsen, J. Fyenbo, K. Larsen and J. Kristensen, *Sol. Energy Mater. Sol. Cells*, 2009, **93**, 422–441.
13 M. Tuomikoski, *Research and Development Activities in Printed Intelligence*, VTT 2006, 21–23.
14 J. M. Ding, A. De la Fuente Vornbrock, C. Ting and V. Subramanian, *Sol. Energy Mater. Sol. Cells*, 2009, **93**, 459–464.
15 D. Zielke, A. C. Hübler, U. Hahn, N. Brandt, M. Bartzsch, U. Fügmann and T. Fischer, *Appl. Phys. Lett.*, 2005, **87**, 123508.
16 V. Marin, E. Holder, M. M. Wienk, E. Tekin, D. Kozodaev and U. S. Schubert, *Macromol. Rapid Commun.*, 2005, **26**, 319–324.
17 C. N. Hoth, S. A. Choulis, P. Schilinsky and C. J. Brabec, *Adv. Mater.*, 2007, **19**, 3973.
18 T. Aernouts, T. Aleksandrov, C. Girotto, J. Genoe and J. Poortmans, *Appl. Phys. Lett.*, 2008, **92**, 033306.
19 R. Tipnis, J. Bernkopf, S. Jia, J. Krieg, S. Li, M. Storch and D. Laird, *Sol. Energy Mater. Sol. Cells*, 2009, **93**, 442–446.
20 Press Release, Konarka Homepage, December 9th, 2008.
21 H. Hoppe and N. S. Sariciftci, *J. Mater. Chem.*, 2006, **16**, 45–61.
22 Y. Kim, S. A. Choulis, J. Nelson and D. D. C. Bradley, *Appl. Phys. Lett.*, 2005, **86**, 063502.
23 W. J. E. Beek, M. M. Wienk and R. A. J. Janssen, *Adv. Funct. Mater.*, 2006, **16**, 1112–1116.
24 C. N. Hoth, P. Schilinsky, S. A. Choulis and C. J. Brabec, *Nano Lett.*, 2008, **8**, 2806–2813.
25 A. Ballantyne, L. Chen, J. Dane, T. Hammant, F. M. Braun, M. Heeney, W. Duffy, I. McCulloch, D. D. C. Bradley and J. Nelson, *Adv. Funct. Mater.*, 2008, **18**, 2378–2380.
26 J. Chang, J. Clark, N. Zhao, H. Sirringhaus, D. W. Breiby, J. W. Andreasen, M. M. Nielsen, M. Giles, M. Heeney and I. McCulloch, *Phys. Rev. B*, 2006, **74**, 115318.
27 P. Schilinsky, U. Asawapirom, U. Scherf, M. Biele and C. J. Brabec, *Chem. Mater.*, 2005, **17**, 2175–2180.
28 Y. Kim, S. Cook, S. M. Tuladhar, S. A. Choulis, J. Nelson, J. R. Durrant, D. D. C. Bradley, M. Giles, I. McCulloch, C.-S. Ha and M. Ree, *Nat. Mater.*, 2006, **5**, 197.
29 S. Malik, T. Jana and A. K. Nandi, *Macromolecules*, 2001, **34**, 275–282.
30 S. Malik and A. K. Nandi, *J. Appl. Polym. Sci.*, 2007, **103**, 2528–2537.
31 H. Sirringhaus, P. J. Brown, R. H. Friend, M. M. Nielsen, K. Bechgaard, B. M. W. Langeveld-Voss, A. J. H. Spiering, R. A. J. Janssen, E. W. Meijer, P. Herwig and D. M. De Leeuw, *Nature*, 1999, **401**, 685.
32 T. Erb, S. Raleva, U. Zhokhavets, G. Gobsch, B. Stühn, M. Spode and O. Ambacher, *Thin Solid Films*, 2004, **450**, 97.
33 M. Koppe, S. Heiml, A. Schausberger, W. Duffy, M. Heeney, I. McCulloch and C. J. Brabec, *Macromolecules*, 2009, accepted.
34 S. H. Chen, A. C. Su, C. S. Chang, H. L. Chen, Derek L. Ho, C. S. Tsao, K. Y. Peng and S. A. Chen, *Langmuir*, 2004, **20**, 8909–8915.
35 W. Ma, J. Y. Kim, K. Lee and A. J. Heeger, *Macromol. Rapid Commun.*, 2007, **28**, 1776–1780.
36 G. Li, V. Shrotriya, J. Huang, Y. Yao, T. Moriarty, K. Emery and Y. Yang, *Nat. Mater.*, 2005, **4**, 864.
37 M. Campoy-Quiles, T. Ferenczi, T. Agostinelli, P. G. Etchegoin, Y. Kim, T. D. Anthopoulos, P. N. Stavrinou, D. D. C. Bradley and J. Nelson, *Nat. Mater.*, 2008, **7**, 158.
38 T. Erb, U. Zhokhavets, H. Hoppe, G. Gobsch, M. Al-Ibrahim and O. Ambacher, *Thin Solid Films*, 2006, **511–512**, 483–485.
39 R. Österbacka, C. P. An, X. M. Jiang and Z. V. Vardeny, *Science*, 2000, **287**, 839–842.
40 V. Zhokhavets, T. Erb, G. Gobsch, M. Al-Ibrahim and O. Ambacher, *Chem. Phys. Lett.*, 2006, **418**, 347–350.
41 S. Yue, G. C. Berry and R. D. McCullough, *Macromolecules*, 1996, **29**, 933–939.
42 C. Waldauf, M. C. Scharber, P. Schilinsky, J. A. Hauch and C. J. Brabec, *J. Appl. Phys.*, 2006, **99**, 104503.

